Electronic Supplementary Material (ESI) for Sustainable Energy & Fuels.
This journal is © The Royal Society of Chemistry 2021

Supporting Information

Porous Graphene-Like MoS_2/Carbon Hierarchies for High-Performance Pseudocapacitive Sodium Storage

Tianhao Yao,[a] Menglong Yao,[a] Hongkang Wang[a,b] *

[a] *State Key Lab of Electrical Insulation and Power Equipment, Center of Nanomaterials for Renewable Energy (CNRE), School of Electrical Engineering, Xi'an Jiaotong University, Xi'an 710049, Shaanxi, China. E-mail: hongkang.wang/mail.xjtu.edu.cn*

[b] *Guangdong Provincial Key Laboratory of Advance Energy Storage Materials, South China University of Technology, Guangzhou, 510640, China*

Experimental section

Materials Characterization. The morphologies of the samples were taken on a FEI Quanta 250F scanning electron microscope (SEM), while the microstructure were measured on a JEOL F200 field emission transmission electron microscope (FE-TEM) with operating voltage of 200 kV. And the high-angle annular dark-field scanning transmission electron microscopy (HAADF-STEM) image and elemental maps were also measured on JEOL F200 with an energy dispersive spectrometer (EDS). A Bruker D2 PHASER X-ray diffraction (XRD)was applied to characterize the phase structure, and chemical compositions and states were measured by X-ray photoelectron spectroscopy (XPS) using an ESCALAB Xi+ Thermo Fisher instrument. The Raman spectra were measured on a Renishaw Raman RE01 scope with a 633 nm excitation Ar laser and thermogravimetric analysis (TGA) was performed on a Mettler thermal analysis TGA/DSC system in air with a temperature ramp of 10 ^{o}C/min. The specific surface area and porous structure of the samples were analyzed according to the Brunauer–Emmett–Teller (BET) method on a SAP 2020 Plus HD88.

Electrochemical Characterization. The sodium storage performance of the as-prepared samples was evaluated as anode materials in CR2025 half cells using sodium metal foil as both reference and counter electrode. In fabrication of working electrode,

70 wt% of the samples (MoS_2/C), 20 wt% of polyacrylic acid (PAA, Mw = 100 000), and 10 wt% of acetylene black were grounded uniformly, using distilled water as the solvent. Then, the as-obtained slurry was then carefully coated on a copper foil, which was subsequently dried in a vacuum oven at 60^{o}C for 12 h. The working electrodes were cut from the coated dopper into disks with a diameter of 14 mm. The adopted electrolyte was 1.0 M $NaClO_4$ in ethylene carbonate/dimethyl carbonate (EC/DMC, 1/1 in volume) with the addition of 5 v% fluoroethylene carbonate (FEC). The cells were assembled in an argon-filled glovebox with both H_2O and O_2 contents less than 1.0 ppm and rested for at least 24 h before tests. Land CT2001A battery test system was applied to obtain Galvanostatic charge/discharge (GCD) results while an Autolab PGSTAT 302N electrochemical workstation were used to run cyclic voltammetry (CV) with the voltage range of 0.01-3 V (vs. Na^+/Na) at various sweep rates from 0.2 to 1.2 mV/s, on which the electrochemical impedance spectroscopy (EIS) was also performed from 10 MHz to 0.01 Hz. All the capacities were calculated based on the active materials.

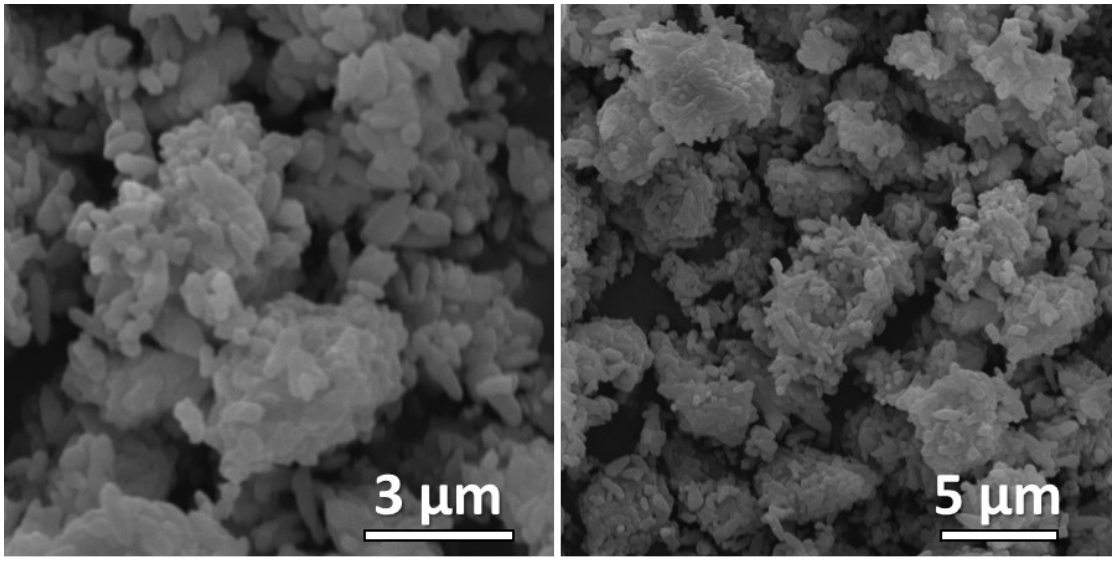

Figure S1. SEM images of $CaCO_3$ templates.

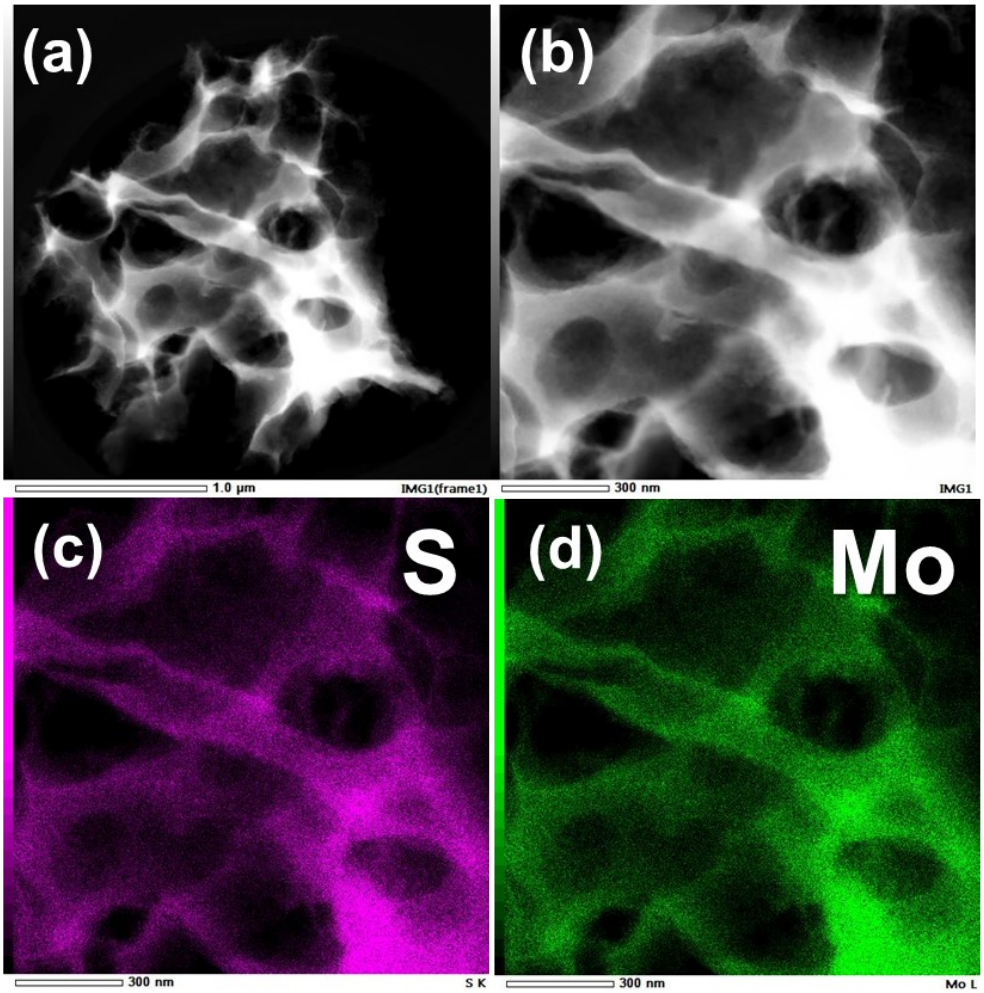

Figure S2. (a-b) HAADF STEM images and corresponding EDS maps of (c) Mo and (d) S.

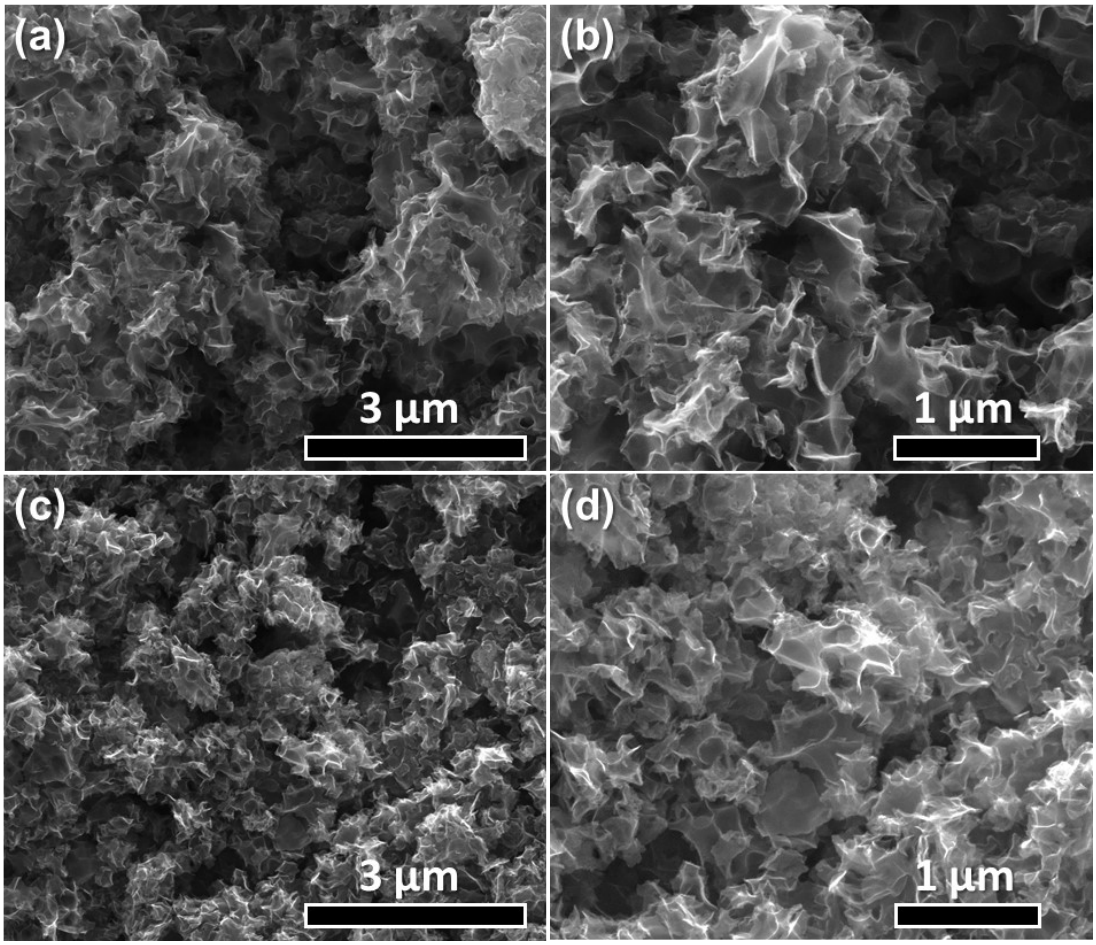

Figure S3. SEM images of (a-b) MoS_2/C50 and (c-d) MoS_2/C150.

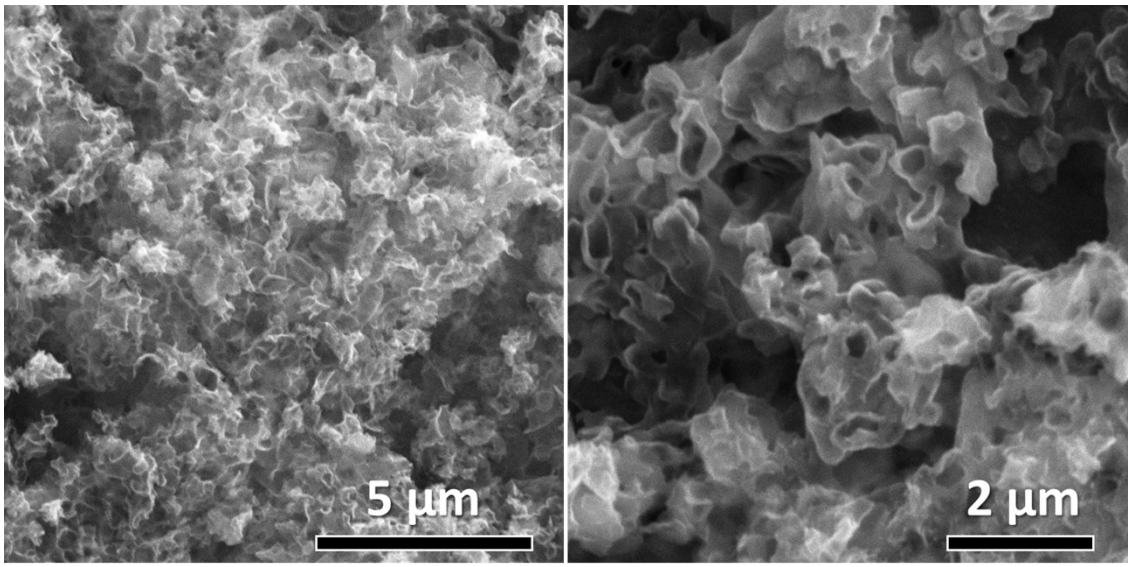

Figure S4. SEM images of N-doped carbon.

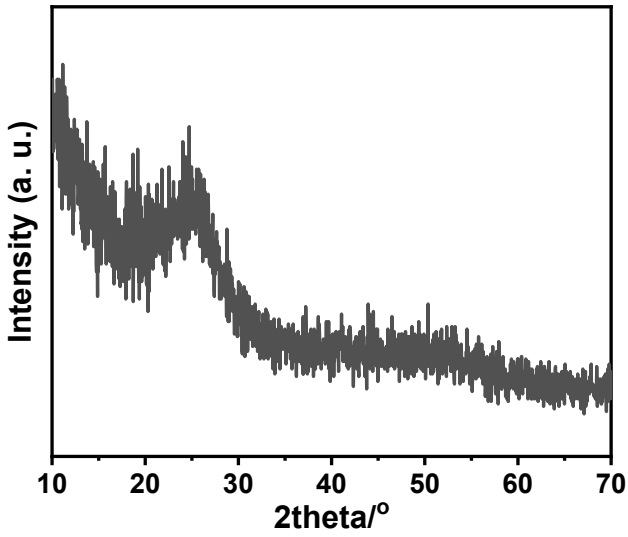

Figure S5. XRD patterns of N-doped carbon.

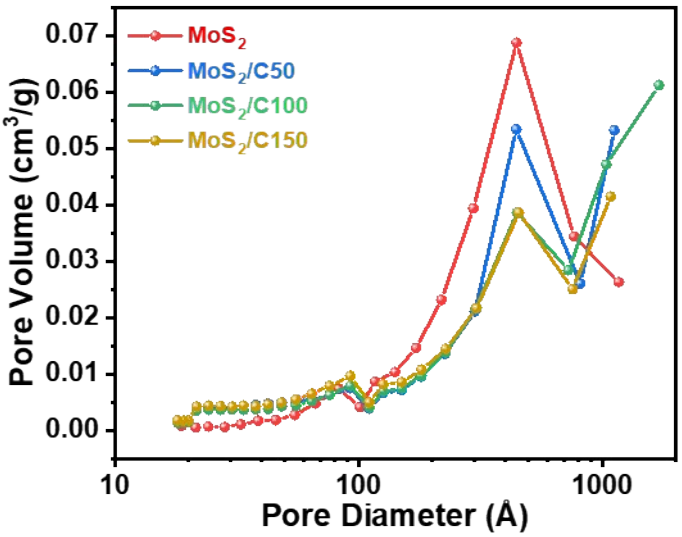

Figure S6. Pore size distribution of MoS_2, MoS_2/C50, MoS_2/C100 and MoS_2/C150.

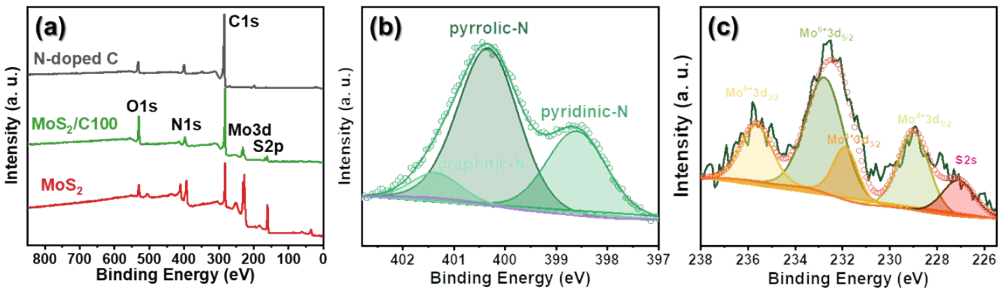

Figure S7. (a) The XPS survey for MoS_2, MoS_2/C100 and N-doped C, (b) N1s XPS spectra for N-doped C and (c) Mo^{6+} 3d XPS spectra for etched MoS_2/C100.

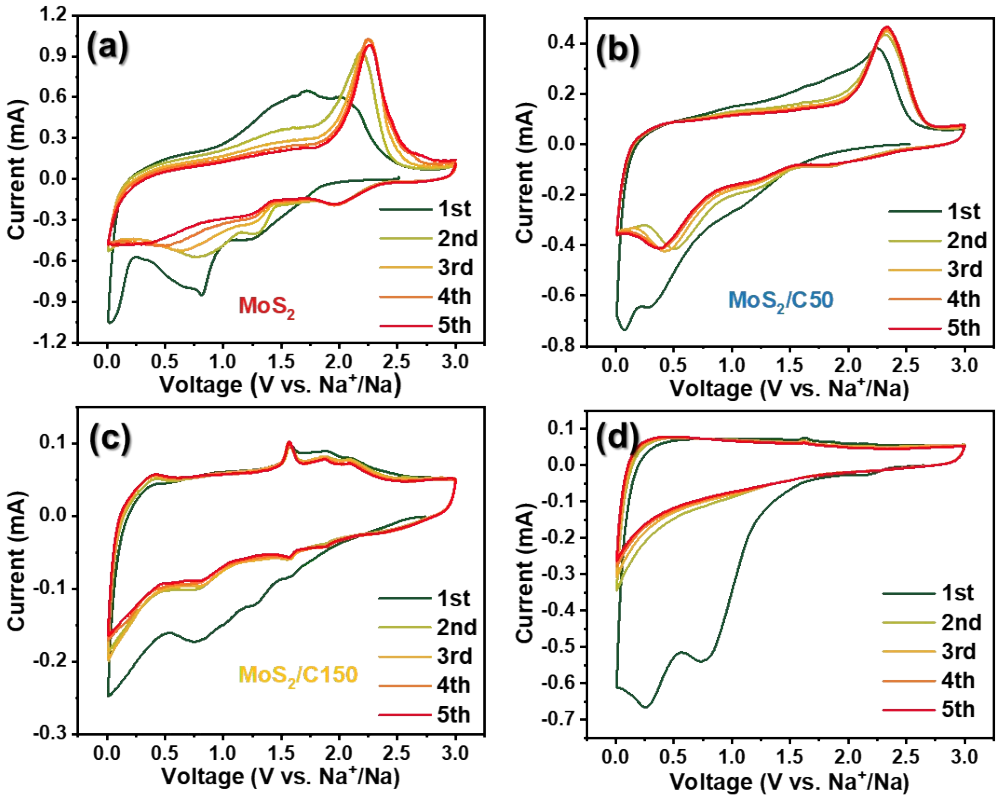

Figure S8. CV curves for (a) MoS_2, (b) MoS_2/C50, (c) MoS_2/C150 and (d) N-doped C at 0.2 mV/s.

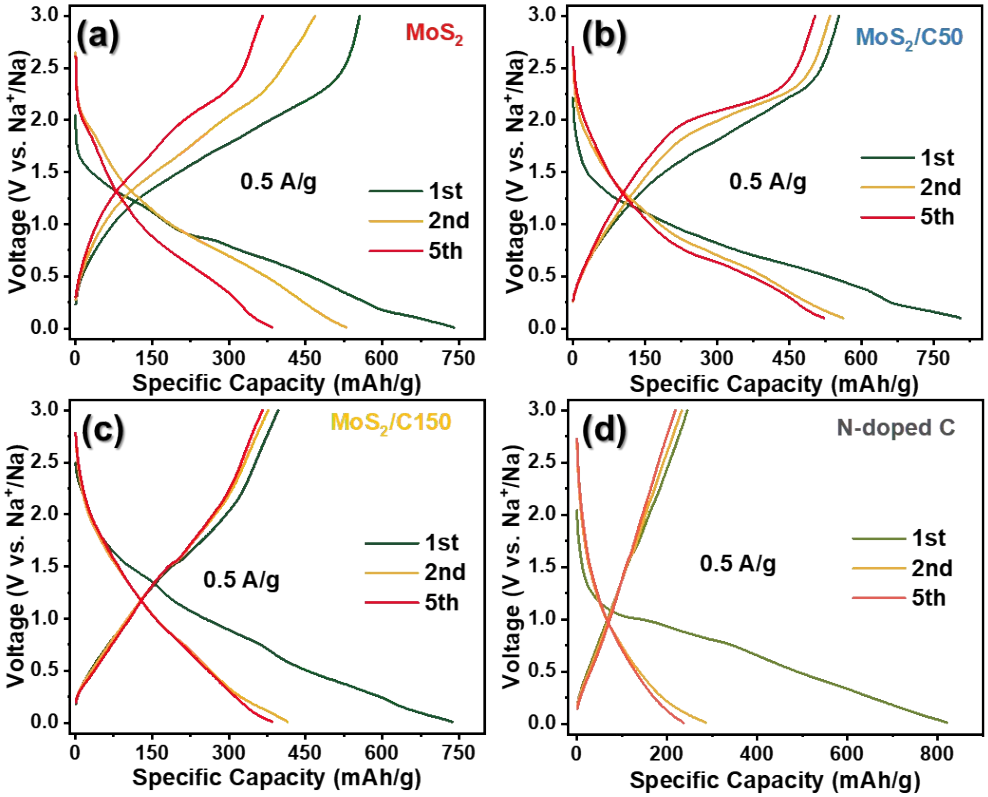

Figure S9. GCD curves for (a) MoS_2, (b) MoS_2/C50, (c) MoS_2/C150 and (d) N-doped C electrodes.

Table S1 The first discharge/charge specific capacities and corresponding ICEs for MoS_2, MoS_2/C50, MoS_2/C100 and MoS_2/C150 electrodes.

Material	**1st discharge capacity(mAh/g)**	**1st charge capacity(mAh/g)**	**ICE**
MoS_2	740	556	75%
MoS_2/C50	805	553	69%
MoS_2/C100	778	459	59%
MoS_2/C150	737	397	54%
N-doped C	820	245	30%

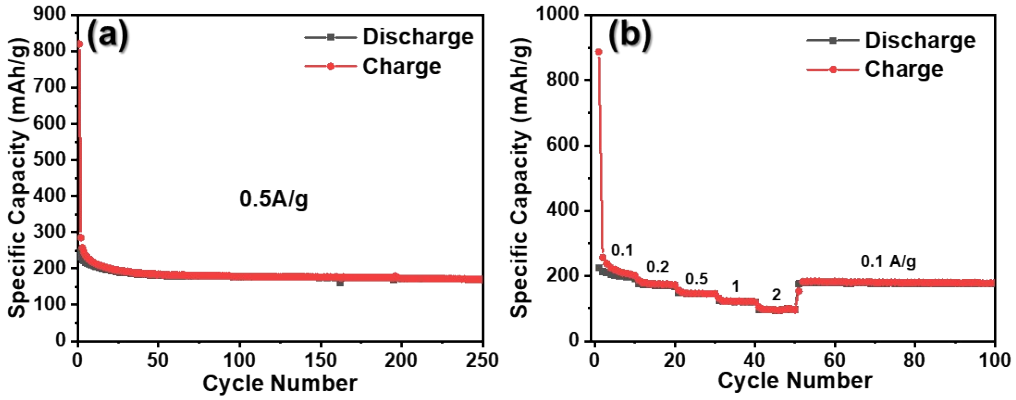

Figure S10. (a) Cycling and (b) rate performance for MoS_2/C150 electrode.

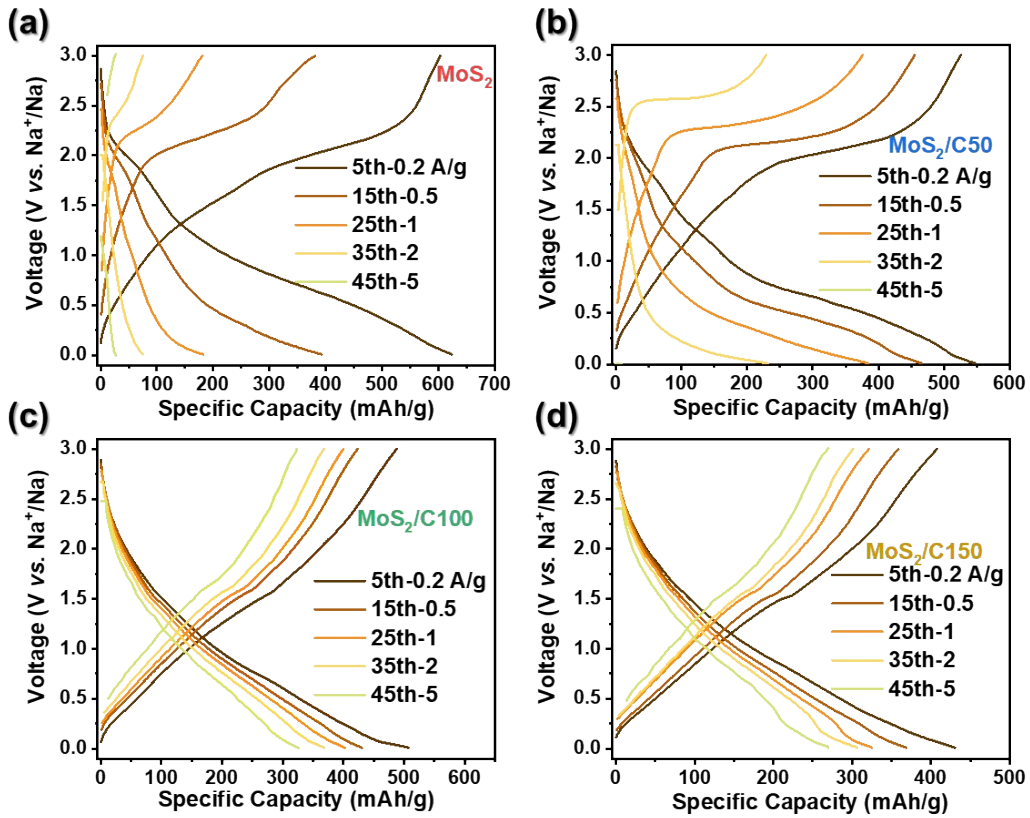

Figure S11. GCD curves at different current densities for (a) MoS_2, (b) MoS_2/C50, (c) MoS_2/C100 and (d) MoS_2/C150 electrodes.

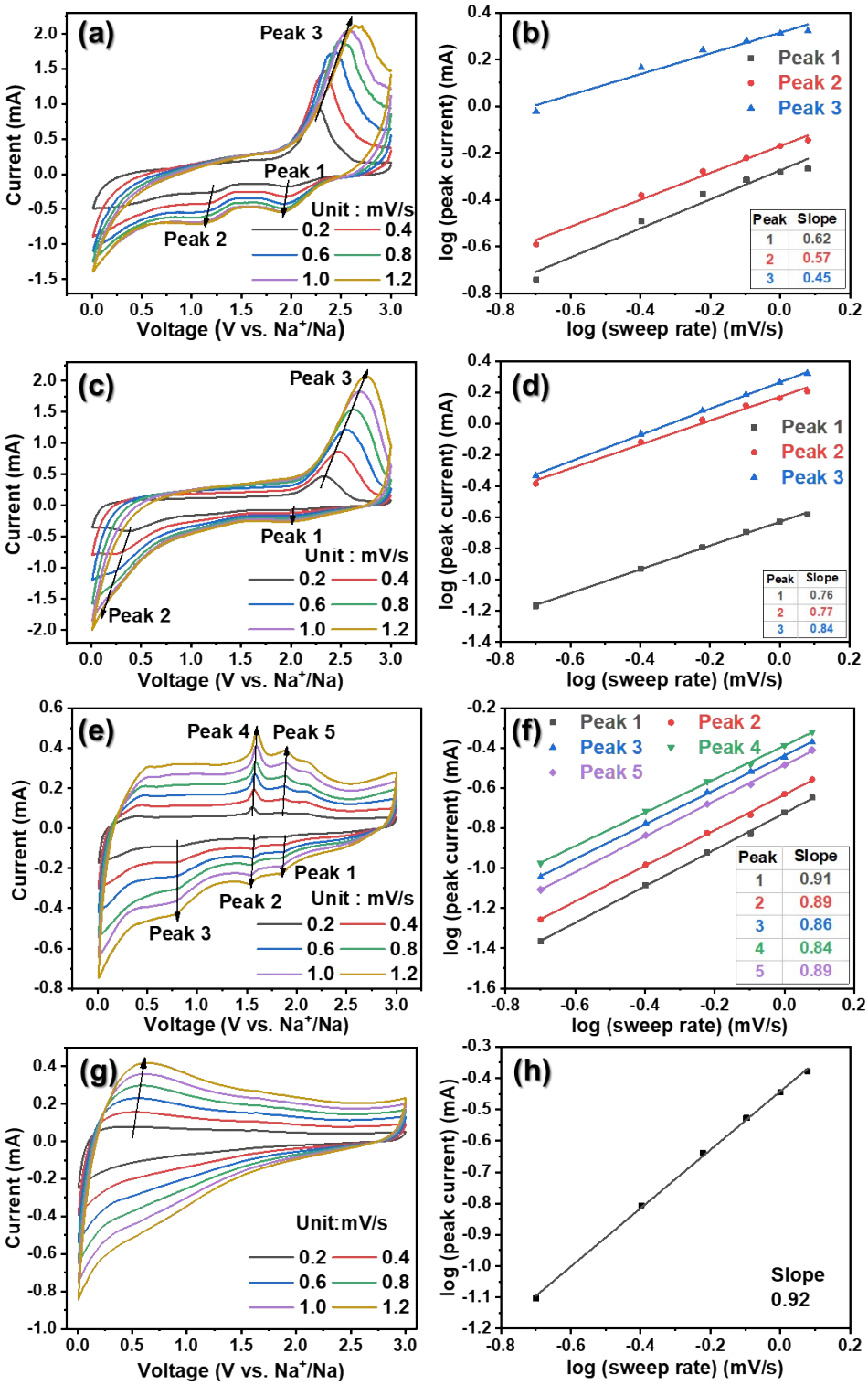

Figure S12. (a, c, e, g) CV curves at different sweep rates and (b, d, f, h) the corresponding log (peak current) vs. log (sweep rate) plots with insets showing the fitted b values for (a, b) MoS_2, (c, d) MoS_2/C50, (e, f) MoS_2/C150 and (g, h) N-doped C electrodes.

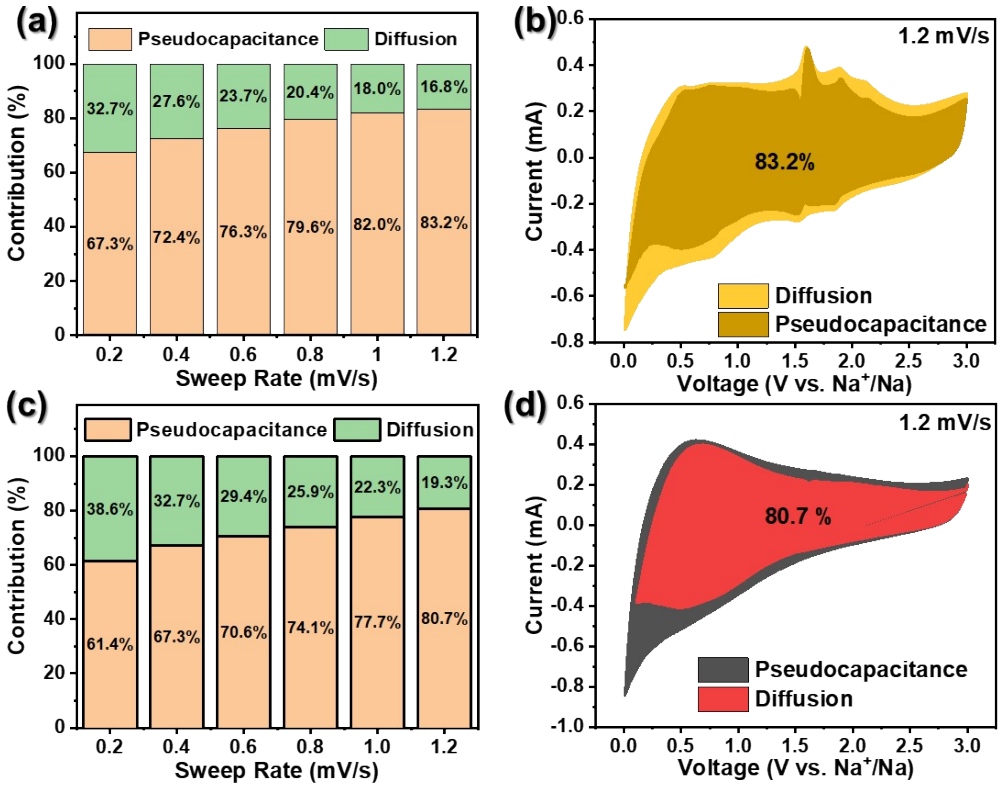

Figure S13. (a, c) Pseudocapacitive contributions at different sweep rates and (b, d) separation of pseudocapacitive and diffusion-controlled contributions of (a, b) MoS_2/C150 and (c, d) N-doped C at 1.2 mV/s.

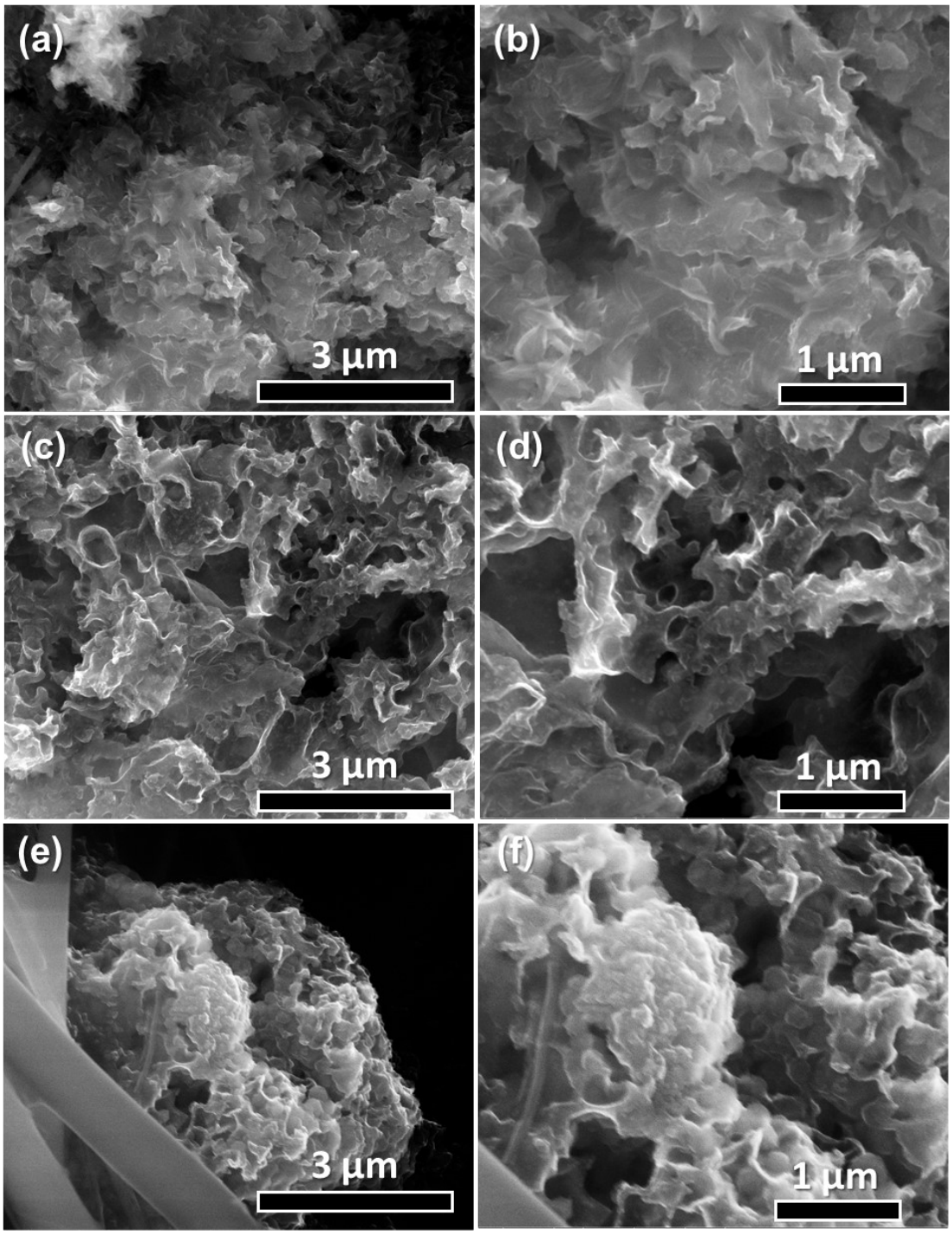

Figure S14. SEM images of charged (a-b) MoS_2/C50, (c-d) MoS_2/C100 and (e-f) MoS_2/C150 electrodes after 300 cycles at 0.5 A/g.

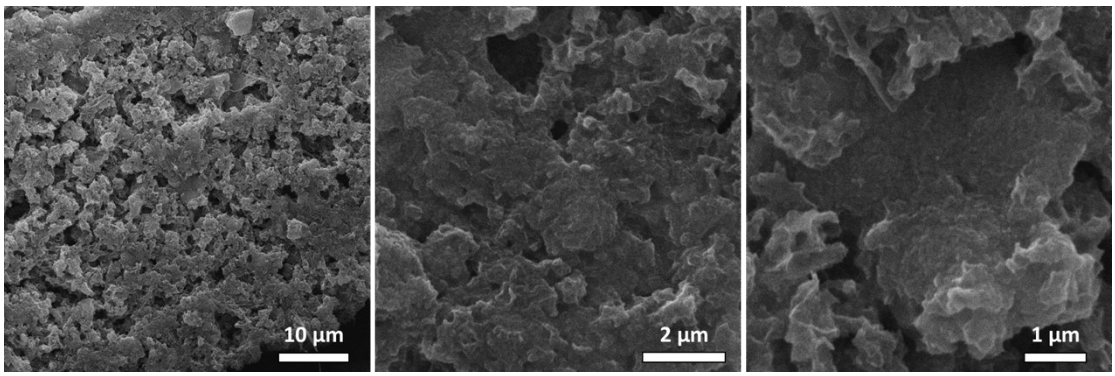

Figure S15. SEM images for bare MoS_2 electrode after 100 cycles.

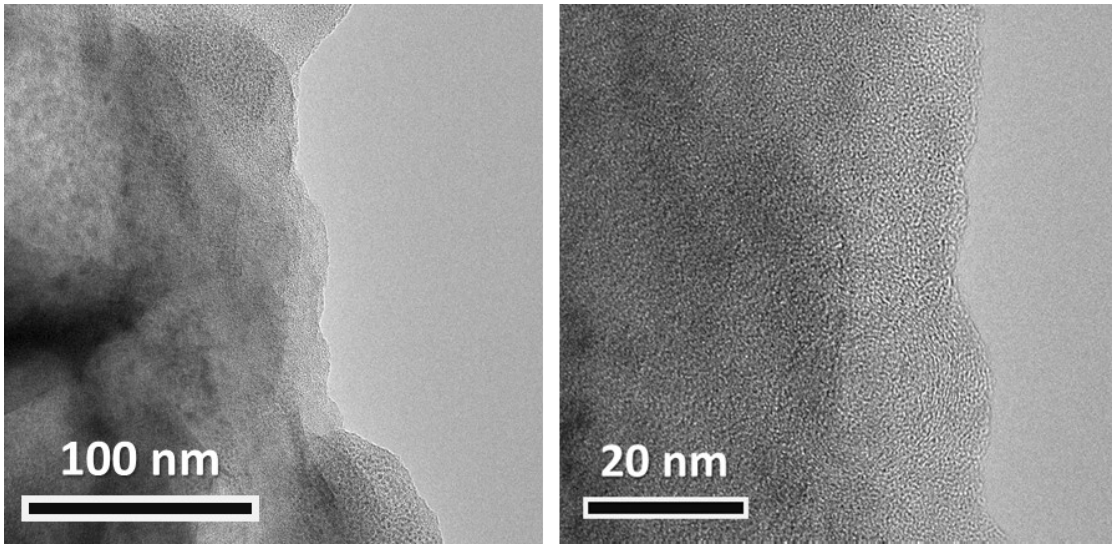

Figure S16. TEM images of charged MoS_2/C150 electrodes after 100 cycles.